

## The Defect Structure of $V_4As_3$

STEN ANDERSSON, HÅKAN ANNEHED, AND LARS STENBERG

*Inorganic Chemistry II, Chemical Centre, University of Lund, Lund, Sweden*

AND ROLF BERGER

*Institute of Chemistry, University of Uppsala, Box 531, S-751 21 Uppsala, Sweden*

Received June 8, 1976

The nature of the defect structure of crystals of  $V_4As_3$  has been studied by electron diffraction and electron microscopy methods. Lattice images reveal that planar defects of the chemical twinning type are common in the orthorhombic  $\alpha$ - $V_4As_3$  crystals. Thermal decomposition, yielding negative crystals, was also studied.

Recently it was shown how the defect structure of alloy-type crystals could be studied using modern electron microscopy methods (1). Crystals of  $Ru_4Si_3$  were shown to be rich in planar defects of the chemical twinning type (2). We now wish to report similar studies of the two forms of  $V_4As_3$  (3, 4).

### Experimental

$\alpha$ - $V_4As_3$  was prepared by chemical transport using iodine, while  $\beta$ - $V_4As_3$  was formed through arc-melting (3). A small portion of the samples was ground under liquid and collected on thin, perforated carbon films and studied in a Philips EM 301 G electron microscope operating at 100 kV. Small single crystals were found which could be aligned with their shortest axis parallel to the electron beam. With a number of (0kl) or (h0l) reflections, respectively, operating for  $\alpha$ - $V_4As_3$  and  $\beta$ - $V_4As_3$ , lattice images were easily observed using objective apertures of 30-80  $\mu$ m.

### Structural Aspects

$\alpha$ - $V_4As_3$  is orthorhombic with the unit cell dimensions  $a = 3.41$  Å,  $b = 13.68$  Å, and

$c = 18.06$  Å. It belongs to the  $Nb_4As_3$  structure type (5).  $\beta$ - $V_4As_3$  is monoclinic with the dimensions  $a = 13.73$  Å,  $b = 3.39$  Å,  $c = 9.23$  Å, and  $\beta = 100.52^\circ$ . It is isostructural with  $Cr_4As_3$  (6). The structure of  $\beta$ - $V_4As_3$  (3) is depicted in Fig. 1 and that of  $\alpha$ - $V_4As_3$  (4) in Fig. 2. As pointed out by Berger (3), the latter structure is formally built up by a twin operation working on the  $\beta$ - $V_4As_3$  structure. The twin plane is indicated by an arrow in Fig. 1. The twinning leads to an unusual coordination polyhedron situated across the twin plane. Chemical twinning normally leads to a change in stoichiometry because

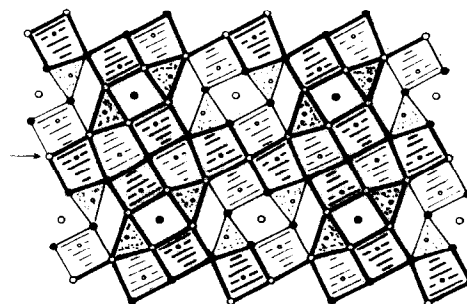


FIG. 1. The structure of  $\beta$ - $V_4As_3$ . Large atoms, vanadium; small atoms, arsenic. All atoms at  $y = 0$  or  $\frac{1}{2}$ . The twin operation plane for obtaining the  $\alpha$ - $V_4As_3$  is indicated by an arrow.

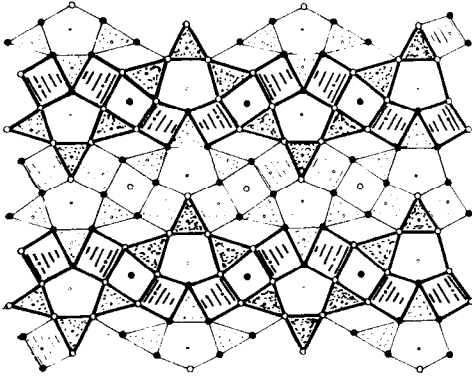


FIG. 2. The structure of  $\alpha$ - $V_4As_3$ . Large atoms, vanadium; small atoms, arsenic. All atoms at  $x=0$  or  $\frac{1}{2}$ .

of the new polyhedra formed across the twin planes, but this is not the case for the  $V_4As_3$  polymorphs. The unit-cell twinning mechanism is analogous to those connecting

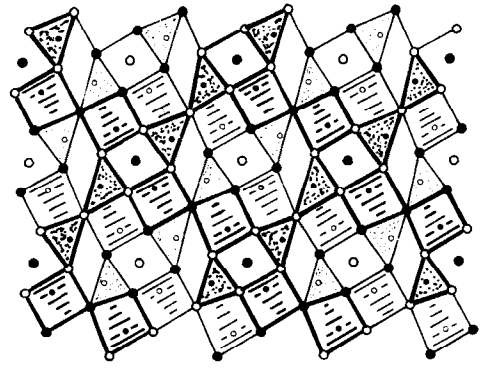


FIG. 3. Hypothetical  $V_3As_2$  structure.

h.c.p. to  $Fe_3C$  and c.c.p. to  $Re_3B$  (2). In view of the close relationship between the two  $V_4As_3$  polymorphs, a planar defect mechanism, involving irregular orientations of the common  $\beta$ - $V_4As_3$  unit, seemed likely.

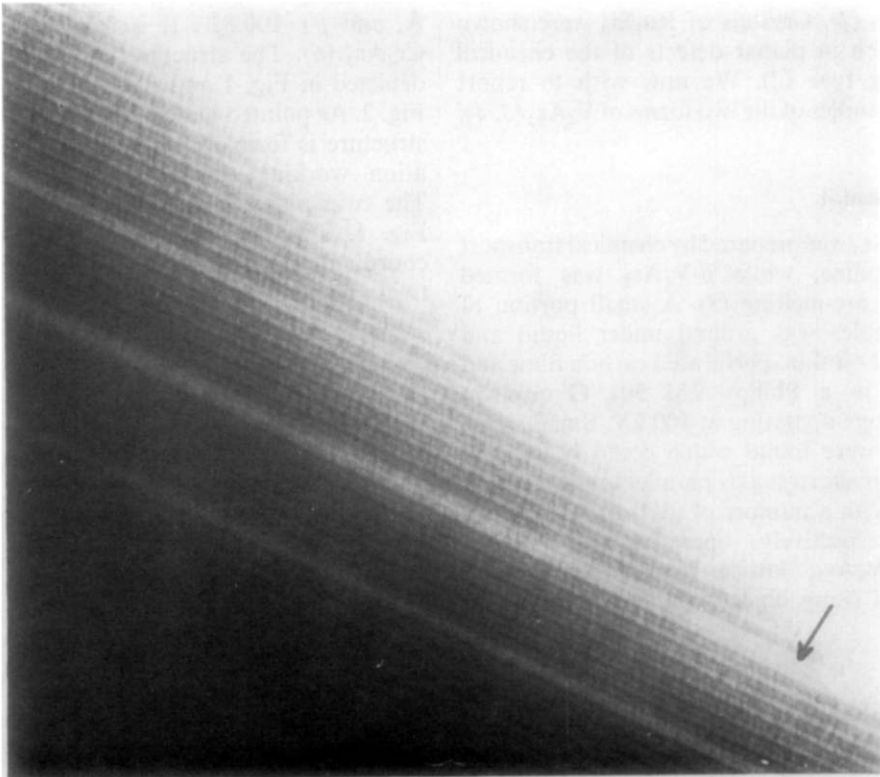


FIG. 4. Lattice image of  $\alpha$ - $V_4As_3$ . The arrow denotes the planar defect explained in Fig. 6.  $\times 1,200,000$ .

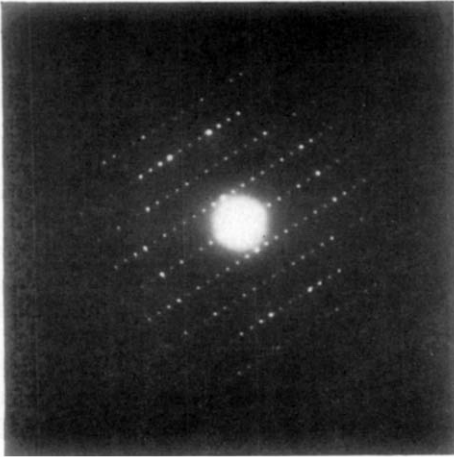


FIG. 5. Electron diffraction pattern corresponding to Fig. 4.

$\beta$ - $V_4As_3$  can be described as being built up of  $AsV_6$  trigonal prisms, interconnected to form sheets, which are infinite in one direction and tied together by cubic body-centered metal units. The prism sheets may be regarded

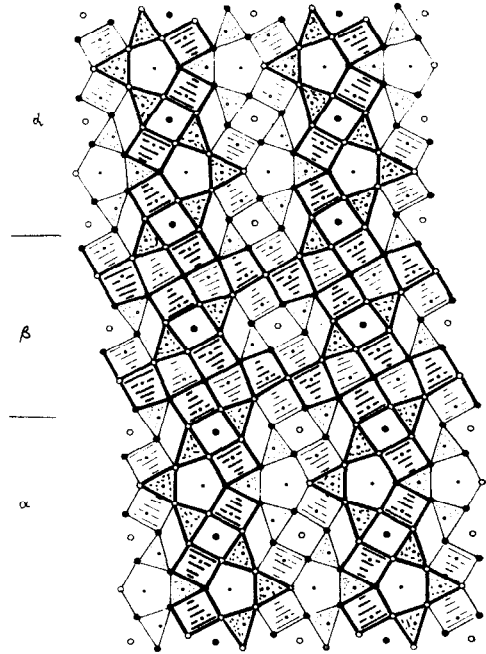


FIG. 6. The atomic structure of the defect region indicated by an arrow in Fig. 4.

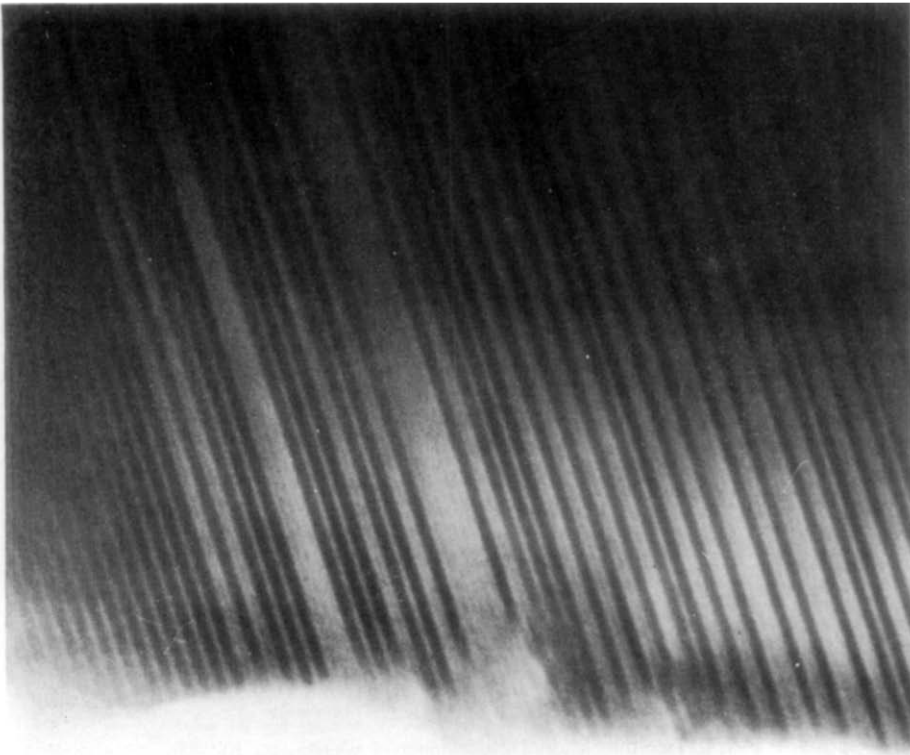


FIG. 7. Extensive disorder in  $\alpha$ - $V_4As_3$ .  $\times 1,200,000$ .

as fragments retained from the parent VAs structure (MnP type). If the width of the sheets in  $\beta\text{-V}_4\text{As}_3$  is extended by another layer of prisms, a hypothetical vanadium arsenide of the composition  $\text{V}_5\text{As}_4$  is obtained. If, on the other hand, the VAs part is reduced by one sheet, the hypothetical structure given in Fig. 3 is obtained. This structure corresponds to the composition  $\text{V}_3\text{As}_2$  and does in fact resemble the true structure of  $\text{V}_3\text{As}_2$ , recently solved (7). A series of hypothetical structures of the composition  $\text{V}_{n+2}\text{As}_{n+1}$  can thus be derived. The figure  $n$  denotes the number of prism sheets tied together without being interlaced with b.c.c. links. The structures with  $n=2$  and  $n=\infty$  are represented by the phases  $\beta\text{-V}_4\text{As}_3$  and VAs, respectively. A defect mechanism in  $\beta\text{-V}_4\text{As}_3$  involving the number of interconnected prism sheets would affect the lattice spacings locally in a crystal and thus be detectable by the lattice-image technique.

### Defect Studies

All the  $\beta\text{-V}_4\text{As}_3$  crystals, aligned and studied by the lattice-image method, revealed constant spacings between the fringes, consistent with stoichiometry and nontwinning.

On the other hand, planar defects were frequently found in  $\alpha\text{-V}_4\text{As}_3$ . Figure 4 shows the edge of a crystal aligned with the electron beam parallel to  $a$ . The corresponding diffractogram is shown in Fig. 5. The regularly repeated unit corresponds to 18 Å, while the spacing between the fringes is 9 Å. The most likely interpretation is that the planar defects observed are untwinned  $\beta\text{-V}_4\text{As}_3$  building blocks. The middle one of the three visible defects running along the crystal obviously corresponds to two such units intervening in the main structure. The detailed atomic structure for this part of the crystal is given in Fig. 6. Each of the other two defects shown in Fig. 4 is similarly explained by just one  $\beta$  unit

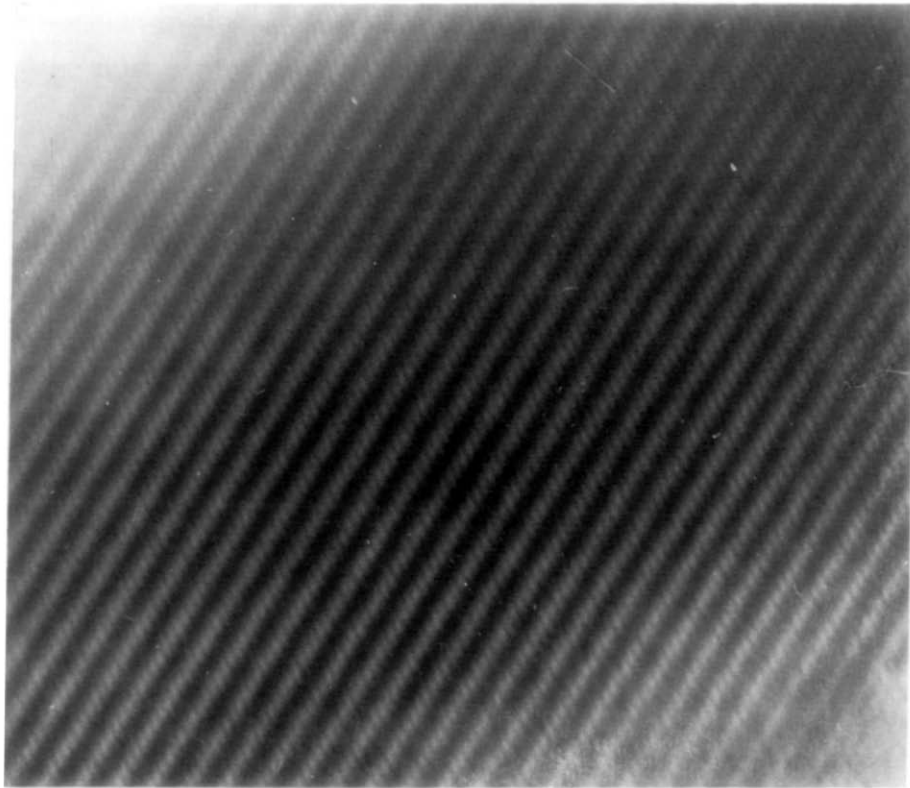


FIG. 8. Two-dimensional lattice image of  $\alpha\text{-V}_4\text{As}_3$ .  $\times 2,300,000$ .

in the  $\alpha$ - $V_4As_3$  matrix. Another example with still more extensive disorder of an analogous kind is shown in Fig. 7.

The resolution and magnification were sometimes increased by lowering the specimen into the objective lens (8). Two dimensional images could then sometimes be recorded, and a typical example is given in Fig. 8. The fringes observed in Fig. 4 are here split up into elongated spots, with an angle of roughly  $125^\circ$ . The two-dimensional lattice image of Fig. 8 can be directly related to the atomic arrangement in the crystal. In Fig. 2, atoms in projection lie approximately on lines forming an angle of  $125^\circ$  with the  $b$ -axis, which agrees well with the angle observed in the micrograph. The elongated spots reflect less dense regions of the structure and give a new example of atomic block resolution. This is similar to the photographs of atomic block resolution

as obtained, for example, by Allpress and Sanders (9) on niobium oxides.

### Decomposition Studies

Crystals of the two forms of  $V_4As_3$  were decomposed in a more intense electron beam than normal. Negative crystals formed rapidly, and their epitaxial orientation to the unit cell of the parent crystal is shown in Fig. 9. The shortest axes of the unit cells were always kept parallel to the electron beam. The negative crystals grew along the shortest axis as well as in a plane perpendicular to the beam. In the case of crystals of  $\beta$ - $V_4As_3$ , growth occurred along  $b$  and parallel to  $a$  and to a diagonal (Fig. 9). When the parent crystals were thin enough for lattice resolution, fringes were observed to peel off, one by one, during the

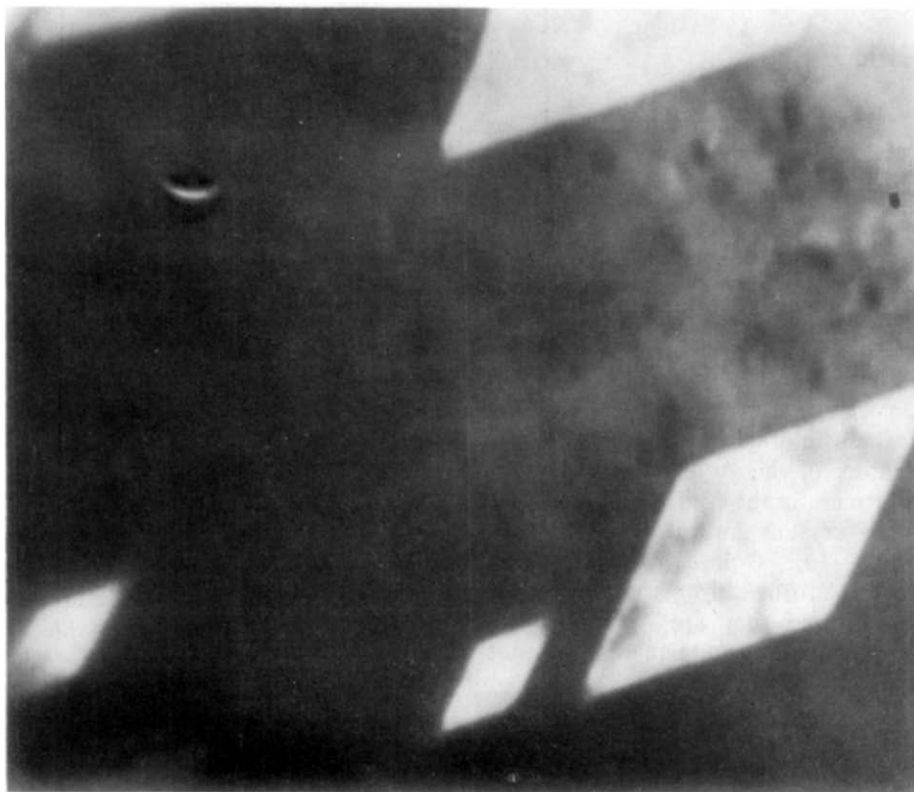


FIG. 9. Typical negative crystals formed during decomposition of a  $\beta$ - $V_4As_3$  crystal. Electron beam parallel to  $b$ .  $\times 860,000$ .



FIG. 10. Negative crystals in  $\beta$ - $V_4As_3$ . Lattice fringes observable in two of the negative crystals. Growth of hexagonally shaped crystals at the edge.  $\times 1,300,000$ .

growth of a negative crystal. When the crystals were too thick for lattice resolution, fringes were often observed after a while, when the negative crystals had penetrated deep enough into the real crystal to make resolution possible, as can be seen in Fig. 10.

The mechanism of decomposition of  $V_4As_3$  and the nature of the atom transport is not clear. Sometimes, in the course of the decomposition, new crystals grew at the edge of the crystal (Fig. 10). Comparatively volatile molecules must form during the decomposition, but whether they are  $As_4$  or species containing both arsenic and vanadium cannot be concluded from this study.

## References

1. S. ANDERSSON, C. LEYGRAF, AND T. JOHNSON, *J. Solid State Chem.* **14**, 78 (1975).
2. S. ANDERSSON AND B. G. HYDE, *J. Solid State Chem.* **9**, 92 (1974).
3. R. BERGER, *Acta Chem. Scand.* **A28**, 771 (1974).
4. K. YVON AND H. BOLLER, *Monatsh. Chem.* **103**, 1643 (1972).
5. B. CARLSSON AND S. RUNDQVIST, *Acta Chem. Scand.* **25**, 1742 (1971).
6. H.-E. BAURECHT, H. BOLLER, AND H. NOWOTNY, *Monatsh. Chem.* **101**, 1696 (1970).
7. R. BERGER, University of Uppsala, to appear.
8. S. IJIMA, *Acta Crystallogr.* **A29**, 18 (1973).
9. J. G. ALLPRESS AND J. V. SANDERS, *J. Appl. Crystallogr.* **6**, 165 (1973).